In-medium modifications of the ω meson

Mariana Nanova for CBELSA/TAPS Collaboration

II. Physikalisches Institut, Universitaet Giessen, D-35392, Germany

Abstract. We have investigated the in-medium modifications of ω mesons in photoproduction experiments using the Crystal Barrel(CB)/TAPS detector system at the ELSA accelerator facility in Bonn. ω-mesons were reconstructed using the $\omega \to \pi^0\gamma$ channel. In a first analysis of the data set on a Nb target, published by D. Trnka et al. [1], evidence for an in-medium mass shift of the ω-meson was deduced from the observed ω lineshape. The signal shape is, however, sensitive to the background subtraction and fitting procedure as pointed out in the literature [2, 3]. For this reason a re-analysis of the same data set was initiated with the goal to reduce the background and to deduce the shape and the absolute magnitude of the background directly from the data. Here we present recent results from this re-analysis. The omega signal resulting after background subtraction has been compared to different scenarios of Gi-BUU transport model calculations for the full incident photon energy range (900-2200 MeV) and near the production threshold (900-1400 MeV).

INTRODUCTION

Experimental studies of in-medium properties of hadrons are motivated by many theoretical investigations based on the expectation of a partial restoration of chiral symmetry at high temperature or increasing nuclear densities. The main goal of the measurements is to study the effect of surrounding strongly interacting matter on the mass and width of hadrons. Most of the recently published results claim a broadening but no mass shift of vector mesons in the medium [4]. As pointed out in [4], the experimentally determined mass distribution represents a convolution of the hadron spectral function with the branching ratio $\Gamma_{H \to X_1 X_2}/\Gamma_{tot}(m)$ into the channel being studied. Since this branching ratio depends on the invariant mass m this may lead to deviations of the experimentally determined mass distribution from the true spectral function. In addition it is demonstrated that for a strong in-medium broadening of the hadron - as observed for the ω meson [5] - contributions from higher densities are suppressed by order $1/\rho^2$, thereby reducing the sensitivity of the ω signal shape to in-medium modifications. Here, we present our investigations of in-medium modifications of the ω meson and discuss the sensitivity of the experiment in different regions of the incident photon energy.

EXPERIMENTAL SETUP

Data have been taken with the detector system Crystal Barrel (CB) [6] and TAPS [7] at the electron stretcher facility ELSA [8, 9]. The detector setup is shown schematically in figure 1(left). Electrons extracted from ELSA hit a primary radiation target, a thin copper or diamond crystal, and produce bremsstrahlung [10]. Photons were tagged in the energy range from 0.5 GeV up to 2.6 GeV for an incoming electron energy of 2.8 GeV. The total tagged photon intensity was about $10^7 \ s^{-1}$ in this energy range.

The Crystal Barrel detector, a photon calorimeter consisting of 1290 CsI(Tl) crystals (≈ 16 radiation lengths), covered the complete azimuthal angle and the polar angle from 30° to 168°. The Nb target in the center of the CB (1 mm thick, 30 mm in diameter) was surrounded by a scintillating fibre-array to detect charged particles [11]. The CB was combined with a forward detector - the TAPS calorimeter - consisting of 528 hexagonal BaF$_2$ crystals ($\approx 12 \ X_0$), covering polar angles between 5° and 30° and the complete 2π azimuthal angle. In front of each BaF$_2$ module a 5 mm thick plastic scintillator was mounted for the identification of charged particles. The combined CB/TAPS detector covered 99% of the full 4π solid angle. The high granularity of this system makes it very well suited for the detection of multi-photon final states. The acceptance for the $p\pi^0\gamma$ channel as a function of mass and momentum of the $\pi^0\gamma$ pair is shown in figure 1(right).

705
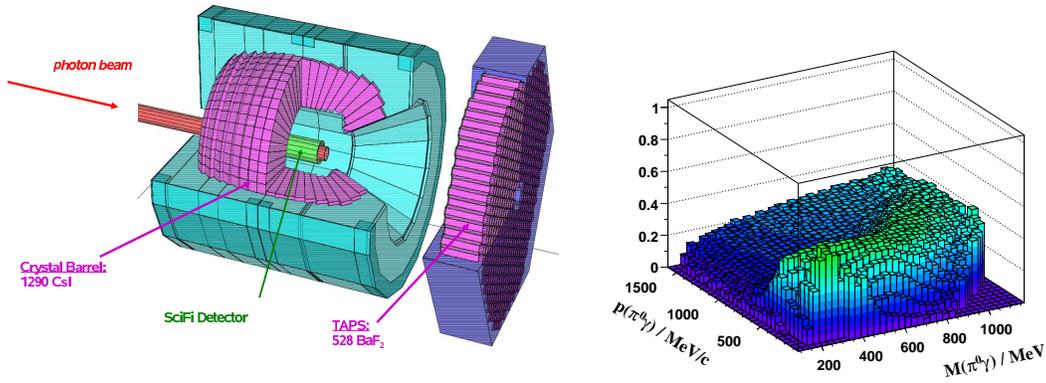
FIGURE 1. (left) The CBELSA/TAPS setup. The electron beam enters from the left, hits the radiator and produces bremsstrahlung. The tagged photons hit the nuclear target, in the center of the Crystal Barrel detector. The TAPS detector serves as a forward wall of the CB. Charged particles leaving the target are identified in the inner scintillating-fibre detector and in the plastic scintillators in front of each BaF_2 crystal in TAPS. (right) Detector acceptance for $p\pi^0\gamma$ final state in the photon energy range 900 to 2200 MeV .

EXPERIMENTAL APPROACH

Reconstruction of the ω meson

The ω meson was reconstructed and identified via the three photon final state invariant mass. According to the relation

$$E^2 = m^2 + p^2 \tag{1}$$

and thus:

$$m_\omega = \sqrt{(E_{\gamma 1} + E_{\gamma 2} + E_{\gamma 3})^2 - (\overrightarrow{p}_{\gamma 1} + \overrightarrow{p}_{\gamma 2} + \overrightarrow{p}_{\gamma 3})^2} \tag{2}$$

Since the ω meson decays according to $\omega \to \pi^0\gamma \to \gamma\gamma\gamma$, the reconstructed particle can only be an ω meson if two of the three photons come from the π^0 decay.

The incident beam energy covered the range of 900 to 2200 MeV, i.e. starting about 200 MeV below the ω production threshold off the free nucleon, which is $E_{\gamma,thresh}$=1107 MeV. However, for coherent ω production off a nuclear target the threshold decreases to $E_{\gamma,thresh}$ = 785.5 MeV for a Nb target, i.e. the threshold is even lower than 900 MeV. The choice of the incident energy interval represents a compromise between sufficiently low energies for ω production off a nuclear target and sufficient discrimination of background sources, which strongly increase with decreasing photon energies.

Only ω mesons decaying inside the nucleus carry information on in-medium properties which are to be studied. To enhance the in-medium decay probability, the vector meson decay length should be comparable to the nuclear radius. This was achieved in the analysis by applying a kinematic cut on the three momentum of the ω meson $|\overrightarrow{P}|_\omega < 500$ MeV/c. But still, only a fraction of the ω mesons will decay inside the nucleus. Thus, one expects the $\pi^0\gamma$ invariant mass spectra to show a superposition of decays outside of the nucleus at the vacuum mass with a peak position at 782 MeV/c^2 and of possibly modified decays inside the nucleus.

The disadvantage of reconstructing the ω meson in the decay mode $\omega \to \pi^0\gamma$ is a possible rescattering of the π^0 meson which was studied in [12]. The authors have demonstrated that the constraint on the kinetic energy $T_{\pi^0} > 150$ MeV suppresses the final state interaction down to the percent level in the invariant mass range of interest.

706
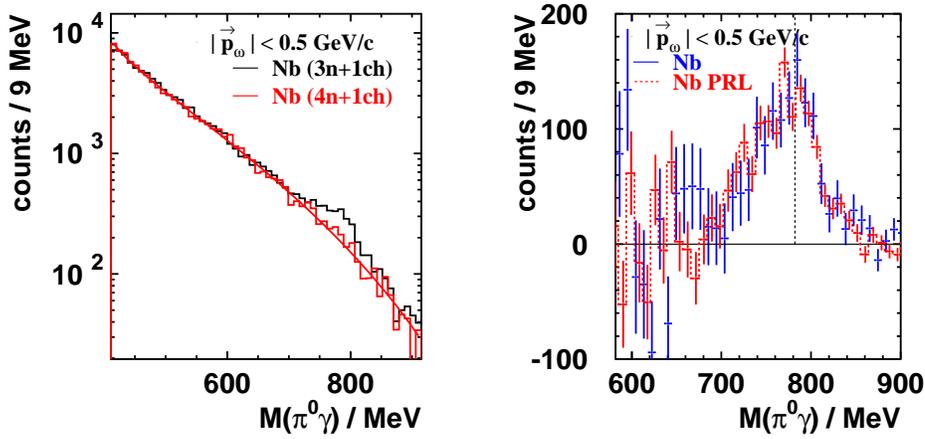
FIGURE 2. (left)The $\pi^0\gamma$ signal spectrum and normalised background spectrum for the Nb target. The solid curve represents a fit to the background distribution. (right) The ω signal published in [1] compared and normalised to the ω signal from this analysis. The spectra are without cut on the pion kinetic energy.

Background Analysis

The next main point in the analysis was the determination of the background from the data and its absolute normalisation. The most probable sources of background come from the reactions $\gamma p \rightarrow \pi^0\pi^0 p$ and $\gamma p \rightarrow \pi^0\eta p$ with 4 γ and one proton in the final state. Due to detection inefficiencies one of the four photons may not be detected, thereby giving rise to a $\pi^0\gamma$ final state, which is exactly identical and therefore not distinguishable from the ω meson final state. To study this background 4 neutral and 1 charged particle from 5 cluster events were selected. One of the four neutral particles was randomly omitted and from the remaining photons a π^0 was identified and combined with the 3rd photon. The $\pi^0\gamma$ invariant spectra and the background spectra after normalisation are shown in fig. 2(left). The absolute height of the background is determined by scaling the counts under the signal and background spectra in the mass range 400 to 960 MeV, excluding the ω peak counts which account for only 2% of the intensity in the spectrum. The spectra are thus normalised without paying special attention to the signal region. Fig. 2(left) shows that the background, which has been directly derived from the data, follows the background shape in the $\pi^0\gamma$ spectrum. The subtraction of the background from the signal spectrum leads to the ω signal shown in fig. 2(right) where it is compared with the final result of the previous analysis [1]. Only slight differences are observed. For a quantitative comparison both signals were fitted with the function:

$$f(x) = A exp[-0.5(\frac{logq_x}{d})^2 - d^2] \tag{3}$$

where

$$q_x = 1 + \frac{(x - E_p)}{\sigma} \cdot \frac{sinh(d \cdot \sqrt{log4})}{\sqrt{log4}} \tag{4}$$

Here A is the amplitude of the signal, E_p is the peak energy, σ is FWHM/2.35 and d the asymmetry parameter. This function takes into account the tail in the region of lower invariant masses due to the energy response function of the detector system. With this fit procedure the widths of the ω signals in this analysis and in [1] have been determined to σ=31.4$\pm$ 3.2 MeV and σ=37.6 $\pm$ 2.5 MeV, respectively (fig. 3). The latter value deviates from the width σ=28.4 $\pm$ 1.0 MeV determined for the LH_2 target which was taken as evidence for an in-medium mass shift of the ω meson in [1]. The width determined in the re-analysis overlaps within errors with the value for the LH_2 target. The evidence for an in-medium ω mass shift can thus not be confirmed.

Cut on the π^0 kinetic energy. To suppress the contribution of the rescattered π^0 a cut on the kinetic energy $T_{\pi^0} >$ 150 MeV has been applied on the $\pi^0\gamma$ and the background spectrum derived from 3 neutral and 1 charged particles.
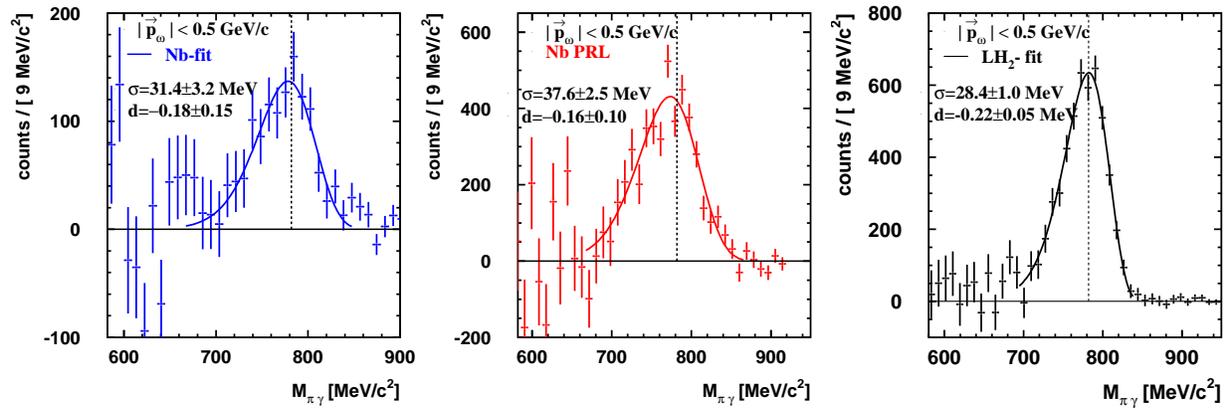
FIGURE 3. *left*: ω signal from this analysis with fit (see the text); *middle*: ω signal from previous analysis published in [1]; *right*: ω signal with fit of the *LH*$_2$ data.

The fit of the Nb data in this analysis yields σ=24.7± 3.1 MeV compared to σ=24.6 ± 1.0 MeV for the *LH*$_2$ target (fig.4 left). In this case there is obviously no evidence for an in-medium mass shift of the ω-meson.

Comparison to Gi-BUU model calculations

A comparison of the ω spectrum for the incident photon energy range 900-2200 MeV with Giessen BUU transport model simulations [13] is shown in fig. 4(left). In this model calculation it is assumed that the in-medium ω pole mass is modified as a function of the probed density and parametrized as:

$$m_\omega^* = m_\omega^0(1 - 0.16\frac{\rho_N}{\rho_0}) \tag{5}$$

The in-medium width increases linearly as a function of the density. The detector resolution (σ=24 MeV) is taken into account. As pointed out by [13], for higher energies 1500-2200 MeV the three scenarios, namely without in-medium modifications, broadening only, and broadening with additional mass shift($\alpha = -0.16$), do not lead to distinguishable differences in the ω lineshape. The data points are in agreement with the Gi-BUU simulations prediction with broadening and mass shift, but also in agreement with the *LH*$_2$ data (fig. 4 left). This contradiction makes the results inconclusive for incident photon energies 900-2200 MeV. Due to the strong broadening of the ω meson observed in a transparency ratio measurement [5] the intensity of in-medium $\omega \to \pi^0\gamma$ signal is suppressed [4]. As a consequence, the ω signal shape becomes less sensitive to a possible mass shift. A significant effect is, however, predicted close to the ω production threshold of E_γ=1107 MeV by the Gi-BUU model [13].

ω meson reconstruction close to the production threshold. For an ω analysis in the threshold region a cut on the incident photon energy from 900 to 1400 MeV was applied. For energies below 1400 MeV the statistical significance of the signal decreases dramatically, therefore it was not reasonable to apply an energy cut lower than 1400 MeV. The analysis went through the same steps described in detail in the previous section, including the cut on the kinetic energy of the pion. For this energy range (900-1400 MeV) the cut on the ω momentum is not applied. A slight deviation of the ω line shape from the reference signal on *LH*$_2$ is observed. Agreement is found between the experimental $\pi^0\gamma$ signal and Gi-BUU simulations for collisional broadening only (see fig. 4 right). The calculated curve with additional mass shift (solid curve in fig. 4 right) does not match the experimental data. The difference in the theoretical calculations for the two cases of broadening only and broadening and mass shift is significant in the region of lower ω masses (less than 750 MeV), where the statistics of the experiment are limited. A run with higher statistics near the production threshold has been performed at the electron accelerator MAMI C and is presently being analyzed. According to [14]
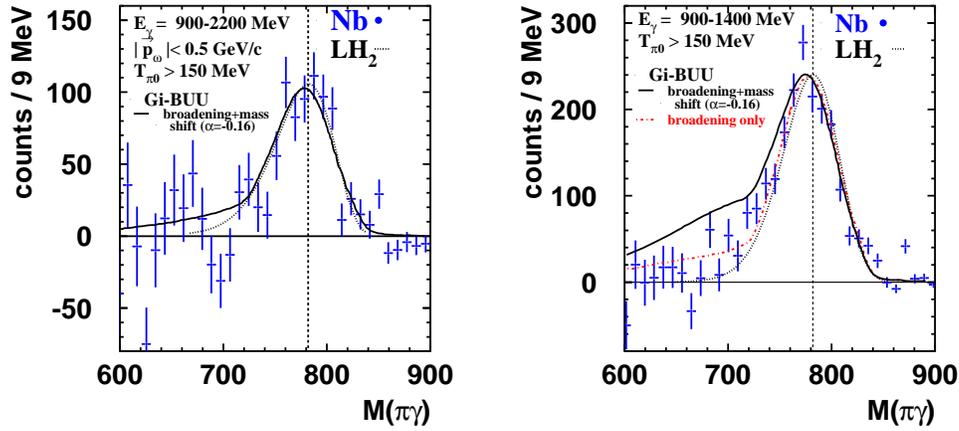
FIGURE 4. ω spectrum on Nb target for E_γ = 900-2200 MeV(left) and for E_γ = 900-1400 MeV(right) compared to the Gi-BUU simulations for E_γ=900-1200 MeV and LH_2 data.

the low mass omega mesons predicted for the broadening only case represent omegas which are produced off shell in the nucleus and decay outside of the nucleus. They are hindered to reach the free omega mass due to the low total energy available.

Conclusion

In conclusion, the ω signal obtained for the full energy range (E_γ=900-2200 MeV) with the $|\vec{P}|_\omega < 500$ MeV/c cut does not allow a discrimination between different in-medium modification scenarios. The near threshold data (E_γ=900-1400 MeV) without momentum cut favour the scenario where only a broadening of the ω meson in the medium has been assumed.

ACKNOWLEDGMENTS

REFERENCES

1. D. Trnka *et al.* CBELSA/TAPS Collaboration, *Phys. Rev. Lett.* **94**, 192303 (2005).
2. E. Hernandez, M. Kaskulov, and E. Oset, *Eur. Phys. J. A* **31**, 245 (2007).
3. E. Oset *et al.*, *Prog. Part. Nucl. Phys.* **61**, 260 (2008).
4. S. Leopold, V. Metag and U. Mosel, *arXiv* **0907.2388** (2009).
5. M. Kottula *et al.* CBELSA/TAPS Collaboration, *Phys. Rev. Lett.* **100**, 192302 (2008).
6. E. Aker *et al.*, *Nucl. Instr. and Methods A* **321**, 69 (1992).
7. R. Novotny *et al.*, *IEEE Trans. Nucl. Sci.* **38**, 392 (1991).
8. D. Husmann, and W. J. Schwille, *Phys. Bl.* **44**, 40 (1988).
9. W. Hillert, *Eur. Phys. J. A* **28**, 139 (2006).
10. D. Elsner *et al.*, *Eur. Phys. J. A* **33**, 147 (2007).
11. G. Suft *et al.*, *Nucl. Instr. Meth., A* **538**, 416 (2005).
12. J. G. Messchendorp, and *et al.*, *Eur. Phys. J. A* **11**, 95 (2001).
13. K. Gallmeister, M. Kaskulov, U. Mosel, and P. Muehlich, *Prog. Part. Nucl. Phys.* **61**, 283 (2008).
14. P. Muehlich, Dissertation, Giessen University, 2007.